ORIGINAL ARTICLE   **Open Access**

LHPP promotes the intracellular reactive oxygen species accumulation and sensitivity of gastric cancer to cisplatin via JNK and p38 MAPK pathways

Kai Gao[1], Ning Yin[1], Zhaolong Shen[1], Qiqing Li[1], Peng Chen[2] and Kaiyan Yang[1]

[1]Department of Gastrointestinal Surgery, The Third Xiangya Hospital of Central South University,

Changsha and [2]Department of General Surgery, The Third Hospital of Zhuzhou, Zhuzhou, Hunan, PR China

Summary. Background. Cisplatin is the first-line chemotherapy drug for the treatment of gastric cancer (GC) patients. However, GC patients who are resistant to cisplatin often do not benefit from it. Therefore, finding a key molecule that affects cisplatin sensitivity is expected to enhance the efficacy of cisplatin in GC treatment.

Methods. The human GC cell lines SGC-7901 and BGC-823 were used. The protein chip array was used to screen the cisplatin-resistance genes from the complete response and non-complete response GC patients' tissues, then, the differential gene expression analysis, GO function annotation analysis, and KEGG pathway enrichment analysis were performed. The GC tissue chip in the GEO database was analyzed to screen the target gene. Flow cytometry, Hoechst 33342 staining assay, Western Blot, MTT, tumor sphere formation, cell cycle, and apoptosis assays were performed to explore the effect of Phospholysine Phosphohistidine Inorganic Pyrophosphate Phosphatase (LHPP) on the apoptosis, stemness, and reactive oxygen species (ROS) accumulation of cisplatin-resistant GC cells treated with cisplatin. *In vivo*, the cisplatin-resistant GC cell lines transfected with pcDNA-LHPP or si-LHPP were injected subcutaneously into mice to construct GC subcutaneous xenograft GC models.

Results. Based on protein chip array and bioinformatics analysis, it was found that LHPP is the core molecule in the cisplatin resistance regulatory network in GC, and its expression is down-regulated in GC cisplatin-resistant tissues and cells. *In vitro* and *in vivo* experimental results show that the up-regulated expression of LHPP is closely related to the increase in sensitivity of GC to cisplatin. Mechanically, we found that overexpression of LHPP may inhibit the activation of the JNK and p38 MAPK pathways, promote cisplatin-induced ROS accumulation, suppress stemness, and enhance the sensitivity of GC to cisplatin.

Conclusions. Up-regulation of LHPP may inhibit the activation of the JNK and p38 MAPK pathways, attenuate stemness, and enhance the accumulation of intracellular ROS, thereby promoting cisplatin-mediated GC cell apoptosis and enhancing cisplatin sensitivity.

Key words: Cisplatin, Phospholysine phosphohistidine inorganic pyrophosphate phosphatase, Gastric cancer, Chemoresistance, Mitogen-activated protein kinase

Introduction

Gastric cancer (GC) is one of the most common malignant tumors of the digestive system in the world. The Global Cancer Statistics 2020 estimated that there were approximately 1,089,103 new cases of GC (the 6th highest incidence of malignant tumors) and 768,793 deaths of GC (the 3rd highest mortality of malignant tumors) in 2020 (Sung et al., 2021). Although the survival of GC has improved markedly compared with 40 years ago, the current 5-year survival rate is still less than 20% (Sexton et al., 2020). The occurrence of chemotherapy resistance increases the resistance of GC cells to chemotherapy drugs, which undoubtedly limits its clinical application (Peng et al., 2020; Zhang et al.,

2021).

Platinum is used as a cornerstone drug for the treatment of GC (Attia and Smyth, 2021). The effective rate of platinum is about 20~50%, and the progression-free survival of platinum is 3~7 months (Arai et al., 2019; Kamimura et al., 2021). However, clinically, there are widespread differences in the efficacy and survival rate of different patients with related chemotherapy regimens. The main reason is primary and secondary drug resistance induced by chemotherapy drugs (Arai et al., 2019). It is worth noting that abnormal gene expression in cancer tissues of different patients may also affect the efficacy of chemotherapy drugs (Arai et al., 2019; Cai et al., 2020; Zhao et al., 2020a,b). Studies have shown that the malignant transformation of malignant tumors is related to chronic oxidative stress, and the level of reactive oxygen species (ROS) in cells undergoing malignant transformation increases drastically (Chiu et al., 2020; Wang et al., 2020a). The level of intracellular ROS production is closely related to cell death (Wang et al., 2020a). Although tumor cells are adaptable to the stimulation of endogenous and continuous oxidative stress, once the ROS level increases above the toxicity threshold, it still leads to cell death (Wang et al., 2020a). A recent study further confirmed that the combination of cisplatin and exogenous drugs can increase the sensitivity of cisplatin-resistant tumor cells to cisplatin (Koken et al., 2020). However, the underlying mechanism of GC cell resistance to cisplatin and the effect of cisplatin-resistant GC cell lines on the accumulation of intracellular ROS and stemness characteristics in GC cells are still unclear.

A recent study has discovered a new kind of tumor suppressor protein phospholysine phosphohistidine inorganic pyrophosphate phosphatase (LHPP) (Hindupur et al., 2018). LHPP is a histidine phosphatase, which has the opposite effect of histidine kinase and can reverse the phosphate group connected to histidine on the protein (Hindupur et al., 2018). Researchers have found that low expression of LHPP can lead to up-regulation of histidine phosphorylation and promote tumor growth (Li et al., 2019; Sun et al., 2020; Wu et al., 2020). The mitogen-activated protein kinase (MAPK) signaling pathway is an important information transmission pathway in cells, which participates in many physiological processes, such as cell growth (Zhu et al., 2020), differentiation (Kurtzeborn et al., 2019), and immune response (Wang et al., 2020b). The MAPK family includes extracellular signal-regulated kinase (ERK), extracellular signal-regulated kinase 5 (ERK5), c-Jun N-terminal kinase (JNK), and the p38 pathway (Kurtzeborn et al., 2019). Studies have found that the MAPK pathway in tumor cells often exhibits dysfunction (Kurtzeborn et al., 2019; Wang et al., 2020b; Zhu et al., 2020). Multiple studies have confirmed that the MAPK pathway is involved in multiple processes such as tumorigenesis (Kurtzeborn et al., 2019; Zhu et al., 2020) and chemotherapy resistance (Lee et al.,

2020). So, are the MAPK pathway and LHPP involved in the cisplatin resistance of GC? What is the relationship between the MAPK pathway and LHPP?

In this study, based on the protein chip array and bioinformatics methods, we first discovered that LHPP is the core molecule in the cisplatin resistance regulatory network of GC, and its expression is down-regulated in cisplatin-resistant cells. *In vitro* and *in vivo* experiments have shown that the up-regulated expression of LHPP is closely related to the increase in cisplatin sensitivity of GC cell lines. Further bioinformatics methods and *in vitro* experiments have found that JNK and p38 MAPK signaling pathways were involved in the biological functions mediated by LHPP. The above results identified a crucial role of LHPP in inhibiting tumor growth and stemness, and promoting intracellular ROS accumulation and the sensitivity of GC cells to cisplatin through JNK and p38 MAPK signaling pathways.

Materials and methods

GC patients inclusion and GC tissue samples collection

Our research plans were approved by the Clinical Research Ethics Committee of the Third Xiangya Hospital of Central South University, Changsha, China (NO.: KS2013-02-0096H), according to the Declaration of Helsinki (as revised in 2013). Informed consent was obtained for experimentation with human subjects. From May 2013 to July 2016, a total of 164 GC tissue samples were collected from patients undergoing GC surgery in the Department of Gastrointestinal Surgery, Third Xiangya Hospital of Central South University, including 71 cisplatin-resistant, 53 cisplatin-sensitive, 10 paclitaxel-resistant, 10 paclitaxel-sensitive, 10 5-fluorouracil-resistant, and 10 5-fluorouracil-sensitive patients. All patients were pathologically diagnosed as GC after surgery. All patients were followed up for 5 years.

Cell culture, plasmid transfection, and small interfering RNA (siRNA) transfection

Human GC cell lines, including KATO III, MGC-803, SGC-7901, GTL16, and MKN-28, were cultured with RPMI-1640 medium containing 10% fetal bovine serum. The culture environment was 37°C, 5% CO_2, and saturated humidity. GC cells in the logarithmic growth phase were inoculated into a 6-well plate and randomly divided into 4 groups (LHPP small interfering RNA (si)-LHPP group, si-negative control (NC) group, LHPP overexpression vector pcDNA-LHPP group, and pcDNA-NC group). The liposome transfection method was used for transfection with Lipofectamine 2000 reagent. The si-LHPP, si-NC, pcDNA-LHPP, and pcDNA-NC were all synthesized by Guangzhou Ribobio Company. The transfection efficiency was detected by the q-PCR method 48h after transfection.

Establishment of cisplatin-resistant GC cell lines

Cisplatin-resistant GC cell lines were established by exposing MGC-803 and SGC-7901 cells to gradually increasing doses of cisplatin (0-32.0 μg/mL) for 4 months. Two weeks after the withdrawal of the cisplatin treatment, the biological characteristics of the resistant GC cell lines were observed. One month after the withdrawal of the cisplatin, the cisplatin-resistant GC cell lines still maintained drug resistance. Compared with the IC50 when the cisplatin was withdrawn, there was no statistical difference in the IC50 change at 1 month after the cisplatin was withdrawn ($P>0.05$), indicating that the cisplatin-resistant GC cell lines have better drug resistance stability.

Protein chip arrays and bioinformatics analysis

The SGC-7901 and SGC-7901/cisplatin cell lines were aspirated from the culture medium, and the culture medium was discarded. After the cell layer was completely dissolved, it was stored at -80°C and transported on dry ice to Shanghai Hujing Biotechnology Co., Ltd. for protein chip array.

We used the DAVID online tool to perform Gene Ontology (GO) function annotation analysis and Kyoto Encyclopedia of Genes and Genomes (KEGG) pathway enrichment analysis on the selected differentially expressed genes. Finally, through the Gene Expression Omnibus (GEO) database, the GC tissue expression profile chip was searched. The GSE94714 GC tissue chip was selected using "gastric cancer" AND "cisplatin" as the search keywords.

3-(4,5-dimethylthiazol-2-yl)-2,5-diphenyl-2H-tetrazolium bromide (MTT) assay

The specific procedures were performed as previously described (Li et al., 2019).

RNA extraction and real-time PCR analyses (qRT-PCR)

The primer sequences used for qRT-PCR were as follows: 5′-GAGGCTGGGATTTGACATCTC-3′ (forward) and 5′-GAGCAGGTATGGTCGCAGG-3′ (reverse) for LHPP; and 5'-AAGGTGAAGGTCGGAG TCA-3' (forward) and 5'-GGAAGATGGTGATGGGAT TT-3' (reverse) for GAPDH (housekeeping gene). The relative level was calculated by the $2^{-\Delta\Delta Ct}$ method.

Fluorescence in situ hybridization (FISH)

The procedure for FISH detection is to place the gastric cancer tissue section on a 37°C constant temperature hot plate, drop 200 μl of pepsin working solution on the section, and digest for 10 minutes. Then, dehydration was performed in gradient ethanol for 2 minutes, and the sections were air-dried naturally. 10 μl of LHPP dual-color probe working solution was dropped on the tissue area to be hybridized on the slice, a cover glass was added, and lightly pressed to make the probe evenly distributed, and the edge was sealed with rubber glue. Sections were placed on a hybridizer, denatured at 85°C for 5 min and hybridized at 37°C for 12h. Finally, 10 μl DAPI dye was added and observed by fluorescence microscope.

Enzyme-linked immunosorbent assay (ELISA)

The supernatant culture medium collected from each group of cells was stored at 4°C. The levels of p-p38, p38, JNK, and p-JNK were measured according to the instructions of the ELISA kit (Wuhan Saipei Biotechnology Co., Ltd., p-p38 item No.: SP91549; p38 item No.: SP91548; JNK item No.: SP91218; p-JNK item No.: SP91200).

Western blot

Total protein was extracted separately from GC cell lines and tissues. Western blot was performed as described before (Sun et al., 2020). The membranes were incubated with antibodies against LHPP (1:500, Santa Cruz Biotechnology Cat# sc-134671, RRID:AB_2012041) and β-actin (1:3000, Miltenyi Biotec Cat# 130-120-277, RRID:AB_2857517). Finally, the secondary antibody was incubated for 2 hours, and the gray band of the protein band was detected by chemiluminescence.

Hoechst 33342 staining assay

GC cells were incubated with 5-ethynyl-20-deoxyuridine (EdU, Shanghai Huicheng Biological Technology Co., Ltd., Shanghai, China) for 5 hours. After three washes with phosphate buffer saline, cells were treated with a $1 \times$ Apollo® reaction cocktail (100 μl/well) for 30 min. After that, each well was stained with Hoechst 33342 (5 μg/ml, 100 μl/well) for 30 min.

Tumor sphere formation

Serum-free medium containing B27 (2%, Invitrogen), human FGF (10μg/ml, Invitrogen), human EGF (10μg/ml, Cell signaling), heparin sodium (2μ/ml, Invitrogen) and methyl cellulose (1%, Invitrogen) was used to suspend GC cell lines. Steady-transformed GC cell lines were seeded in a 24-well ultra-low adhesion plate at a density of 2×10^3 cells per well. Then, the cells were placed in an incubator at 37°C, 5% CO_2 and saturated humidity, and cultured for 10 to 14 days. Then, the number of cloned spheres were counted and pictures taken with an inverted phase-contrast microscope. Each group was designed with three multiple holes. Sphere formation efficiency=the number of cell spheres with a diameter greater than 75um in each well / the total

number of originally seeded cells in each well.

Cell cycle and apoptosis assay

Cell apoptosis was determined by flow cytometry after staining with Annexin V (FITC-conjugated) apoptosis kit. Briefly, GC cell lines were stained with 5 µl Annexin 5-FITC and propidium iodide (PI), respectively, and incubated for 15 min in the dark. Then, The apoptotic cells and cell cycle distribution were analyzed using a flow cytometer.

Detection of intracellular ROS

A total of 1ml of 1×10^7/ml cell suspension was absorbed and 10 nmol 2,7-Dichlorodi-hydrofluorescein diacetate (DCFH-DA, Wuhan Chuqiang Biological Technology Co., Ltd., China) was added. After incubation at 37°C for 30 min, the cells were cleaned with serum-free medium for three times and fluorescence signals were detected by flow cytometry.

Immunohistochemistry

Immunohistochemistry staining was performed on paraffin sections with rabbit monoclonal antibody directed against LHPP (1:100; Santa Cruz Biotechnology Cat# sc-134671, RRID: AB_2012041). The biotinylated goat anti-rabbit secondary antibody (1:5000, Signalway Cat# L3012, RRID: AB_895483) was incubated at 4°C. Finally, the sections were incubated with DAB substrate for 5 min.

Xenografted tumor model

Experiments were performed under a project license (NO.: KS2017-04-0103A) granted by the Ethics Committee of the Third Xiangya Hospital of Central South University, in compliance with the Third Xiangya Hospital of Central South University's guidelines for the care and use of animals. A total of 24 BALB/c nude mice (18-23 g, 5-6 weeks old, 12 male, 12 female) were obtained from Wuhan Chuqiang Biological Technology Co., Ltd., China.

Mice were divided into eight groups according to the random number table method. During logarithmic growth, cells from each of the eight groups (si-LHPP-MGC-803/cisplatin, si-NC-MGC-803/cisplatin, pcDNA-LHPP-MGC-803/cisplatin, pcDNA-NC-MGC-803/cisplatin, si-LHPP-SGC-7901/cisplatin, si-NC-SGC-7901/cisplatin, pcDNA-LHPP-SGC-7901/cisplatin, and pcDNA-NC-SGC-7901/cisplatin) were collected separately. Then, cells were subcutaneously injected into nude mice to establish the xenograft model. After the model was successfully established, cisplatin was injected intraperitoneally at a dose of 3 mg/kg every 3 days for a total of 5 times. The diameter of each xenograft tumor was measured before each administration. The nude mice were sacrificed 3 days after the last dose.

Statistical analysis

The Cytoscape version 3.7.2 (RRID: SCR_003032), R version 3.6.1 (RRID: SCR_002394), and GraphPad Prism version 7.0 (RRID: SCR_002798) software were used in this study. Results were represented as the mean±standard deviation (SD). The differences between normally distributed numeric variables were evaluated by Student's t-test. One-way analysis of variance (ANOVA) was used for the comparison among multiple groups. $P<0.05$ was considered significant.

Results

Characterization of cisplatin resistance in SGC-7901/cisplatin and MGC-803/cisplatin cell lines

Cisplatin cytotoxicity for KATO III, MGC-803, SGC-7901, GTL16, and MKN-28 cell lines was explored. SGC-7901 cells possessed the most sensitivity to cisplatin [half maximal inhibitory concentration (IC_{50})=1.43 µg/ml, Fig. 1A], whereas MGC-803 cells were found to be the least sensitive to cisplatin (IC_{50}=7.16 µg/ml, Fig. 1A). Then, the cisplatin-resistant cell lines (SGC-7901/cisplatin and MGC-803/cisplatin) were established. After exposure to an increasing dose of cisplatin (0-32.0 µg/mL), the IC_{50} values were 15.67±0.47 µg/ml (Fig. 1B) and 29.16±0.53 µg/ml (Fig. 1C) for SGC-7901/cisplatin and MGC-803/cisplatin cells, respectively, showing a 10.81- and 4.15-fold increase as compared to parental cell lines.

Screening of genes related to cisplatin resistance in GC through bioinformatics

We then chose GC tissues from the complete response (CR) or non-complete response (NCR) patients for the protein chip array. A total of 338 differentially expressed genes, including 266 up-regulated genes and 72 down-regulated genes, were explored (Fig. 2A). The enrichment of GO, including biological process (BP), cellular component (CC), and molecular function (MF) subtypes, was shown in Fig. 2B. Then, we searched the interactions between 338 differentially expressed genes related to cisplatin resistance in GC through the STRING database and a PPI network (Fig. 2C). Finally, we screened LHPP as the core gene (Fig. 2D).

Down-regulation of LHPP protein in GC tissue is associated with cisplatin resistance, and suggests a poor prognosis in GC patients

To explore the mechanism of LHPP, we first tested the localization of LHPP in SGC-7901 and MGC-803 cells via FISH assay. The results demonstrated that LHPP was mainly distributed in the cytoplasm of both GC cells (Fig. 3A). The relationship between LHPP

expression and clinical characteristics in GC tissue is shown in Table 1. The low LHPP expression was correlated with poor differentiation, cisplatin resistance, and poor TNM stage. Compared with cisplatin-sensitive
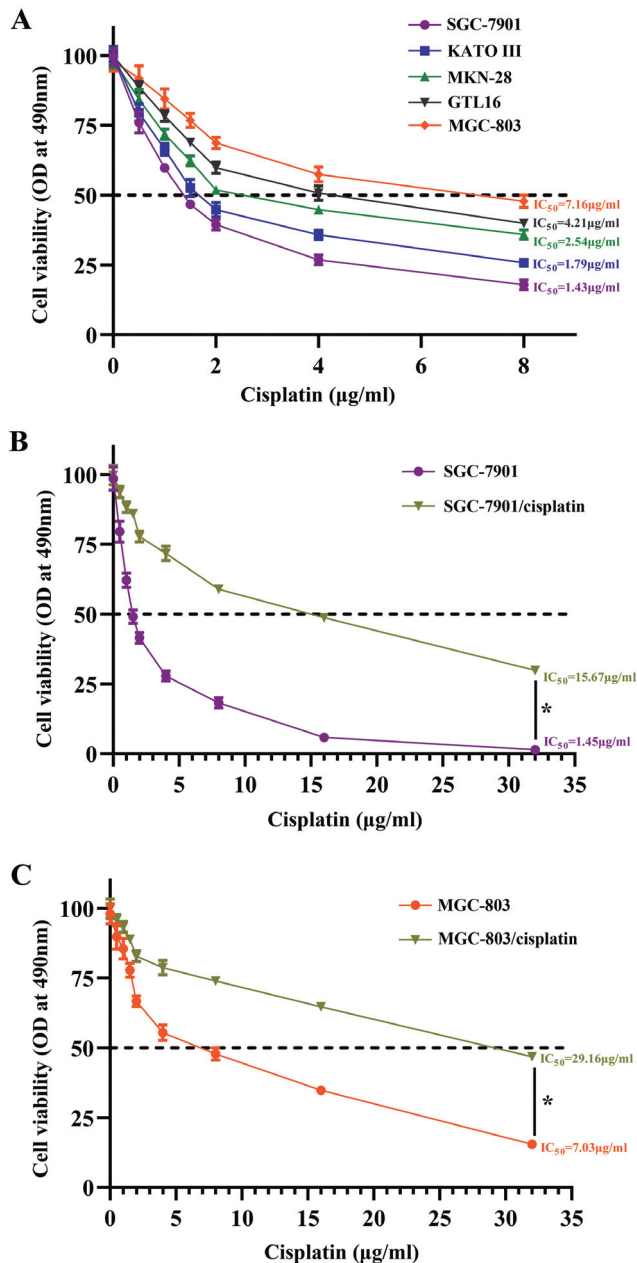
GC tissues, the levels of LHPP protein in cisplatin-resistant GC tissues were significantly lower (Fig. 3B,C). Besides, to reveal the relationship between LHPP down-regulation and patient prognosis, we also investigated the correlation between low LHPP expression and patient survival. After 60 months of follow-up, we found that the 60-month overall survival rates of patients in the low LHPP expression group were notably poorer than those in the high expression group (Fig. 3D). When considering the different sensitivity of GC tissues to cisplatin, we found that compared with high LHPP expression, the 60-month overall survival rate of GC patients with low LHPP expression was significantly decreased in both the cisplatin-sensitive group (Fig. 3E) and the cisplatin-resistant group (Fig. 3F). All the above data revealed that the loss of LHPP expression may promote the resistance of GC tissues to cisplatin and is related to the poor prognosis of GC patients.

Up-regulation of LHPP can promote the sensitivity of SGC-7901/cisplatin and MGC-803/cisplatin cell lines to cisplatin in vitro and in vivo

To further verify the relationship between LHPP expression and GC cisplatin sensitivity, SGC-7901/cisplatin and MGC-803/cisplatin cells were transfected with si-LHPP, si-NC, pcDNA-LHPP, and pcDNA-NC. Different concentrations of cisplatin were given to observe the changes in cell viability. QRT-PCR and Western blot results found that the LHPP expression

Fig. 1. Characterization of cisplatin resistance in SGC-7901/cisplatin and MGC-803/cisplatin cell lines. **A.** Cisplatin cytotoxicity for KATO III, MGC-803, SGC-7901, GTL16, and MKN-28 cell lines was explored. **B.** The IC_{50} for SGC-7901/cisplatin cells. **C.** The IC_{50} for MGC-803/cisplatin cells. * One-way ANOVA was used, and $P<0.05$. Data are expressed as mean±standard deviation. IC_{50}: half-maximal inhibitory concentration; OD: optical density.

Table 1. Correlations between LHPP expression and clinical characteristics in GC patients.

Characteristics	Cases	LHPP expression		χ^2
	(n=124)	High (>Median)	Low (≤Median)	
Gender				0.138
Male	78	40	38	
Female	46	22	24	
Age (years)				0.290
≤60	61	29	32	
>60	63	33	30	
Pathological differentiation grade				12.074
Well	21	16	5	
Moderately	76	39	37	
Poorly	27	7	20	
Sensitivity to cisplatin				35.885
Complete response	53	43	10	
Non-complete response	71	19	52	
TNM Stage				51.321
I, II	75	57	18	
III, IV	49	5	44	
Lymph node metastasis				0.372
Negative	33	15	18	
Positive	91	47	44	

The χ^2 test was used for comparison between groups.

in GC cells transfected with pcDNA-LHPP plasmid was significantly higher than that of the NC group (*P*<0.01, Fig. 4A). Compared with the NC group, SGC-7901/cisplatin and MGC-803/cisplatin cells in the LHPP overexpression expression group were significantly more sensitive to cisplatin (*P*<0.01, Fig. 4B). Then, we achieved LHPP silencing by infecting cells with si-LHPP. Similarly, the opposite results can be observed in the SGC-7901/cisplatin and MGC-803/cisplatin cell lines (*P*<0.01, Fig. 4C,D).
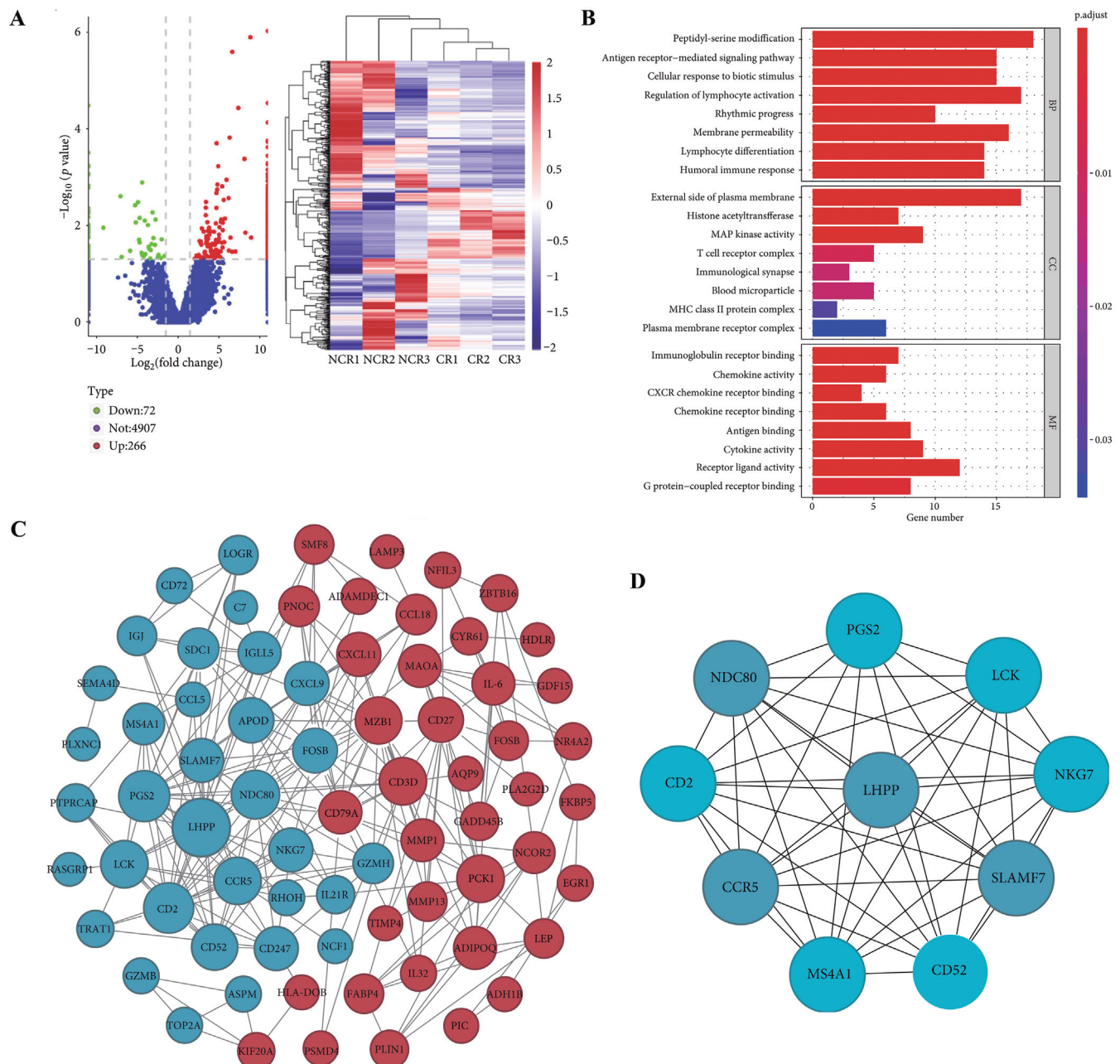

Fig. 2. Protein chip array, volcano map, enrichment analysis, and protein interaction network analysis of differentially expressed genes related to cisplatin resistance in GC. **A.** Protein chip array and volcano map of differentially expressed genes related to cisplatin resistance in GC. The red nodes represent up-regulation, and the green nodes represent down-regulation. **B.** GO enrichment analysis of differentially expressed genes related to cisplatin resistance in GC. **C.** The interaction relationship between the differentially expressed genes is explored by STRING database and a PPI network. **D.** The circles in the network represent the top ten differentially expressed genes (core genes) according to a degree. The darker the color, the higher the degree. BP: biological process; CC: cell components; MF: molecular function; GC: gastric cancer; GO: Gene Ontology; CR: complete response; NCR: non-complete response.

The killing effect of cisplatin is cell apoptosis induced by DNA damage (Zhao et al., 2020a,b). Therefore, to further explore the effect of LHPP on cisplatin sensitivity of GC cells, flow cytometry was performed. We found that overexpression of LHPP enhanced cell apoptosis (Fig. 5,B), nuclear fragmentation (Fig. 6A), and inhibited the capacity to form spheres (Fig. 6B), while down-regulation of LHPP expression had the opposite effect in the SGC-7901/cisplatin and MGC-803/cisplatin cells. In vivo experiments further confirmed the results of cell experiments. The anti-tumor effect of cisplatin on LHPP up-regulated xenograft mice was significantly better, while on LHPP knockdown xenograft mice it was significantly poorer than the control group, indicating that nude mice with high LHPP expression are more sensitive to cisplatin (Fig. 6C-F).

GO and KEGG pathway analyses screen LHPP-associated signal pathways

Then, we sequenced si-LHPP-SGC-7901/cisplatin and si-NC-SGC-7901/cisplatin, and GO and KEGG pathways analyses were performed (Fig. 7). Among differentially expressed genes, down-regulated LHPP was correlated to MAP kinase activity, phosphatase
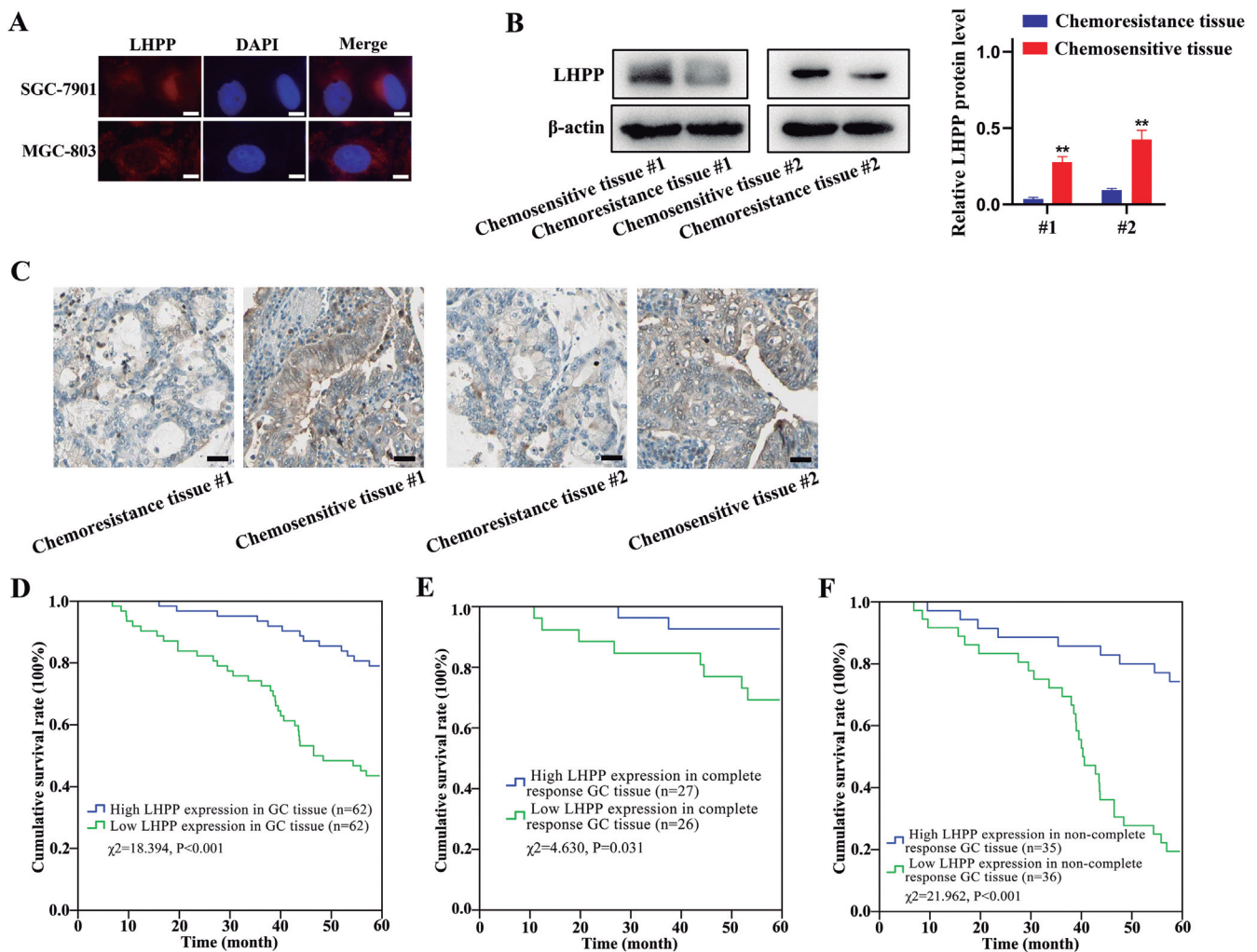

Fig. 3. Down-regulation of LHPP is associated with cisplatin resistance and a poor prognosis in GC patients. **A.** The FISH assay showed that LHPP was mainly distributed in the cytoplasm. **B, C.** Compared with cisplatin-sensitive GC tissues, the levels of LHPP protein in cisplatin-resistant GC tissues were significantly decreased. **D.** The 60-month overall survival rates of patients in the low LHPP expression group were notably poorer than those in the high expression group. Compared with high LHPP expression, the 60-month overall survival rate of GC patients with low LHPP expression was significantly decreased in both the cisplatin sensitive group **(E)** and the cisplatin-resistant group **(F)**. Data are expressed as mean±standard deviation. **$P<0.01$, compared to the control group. GC: gastric cancer; LHPP: phospholysine phosphohistidine inorganic pyrophosphate phosphatase. Scale bar: 50 μm.

binding, transcription factor binding, protein serine kinase activity, and so on (Fig. 7B). Meanwhile, KEGG, a database of gene functions linking genomic information to higher-order functional information, indicated similar results as GO analysis. In detail, the up-regulated genes associated with si-LHPP in GC cells were involved in the MAPK signaling pathway, Toll-like receptor signaling pathway, etc (Fig. 7D). Differentially expressed proteins were defined as those with fold change either over 1.2 or less than 0.83, combined with a fluorescent value greater than 150. Finally, 2 differentially expressed proteins (Table 2) were selected for validation in the following experiment by western blot.
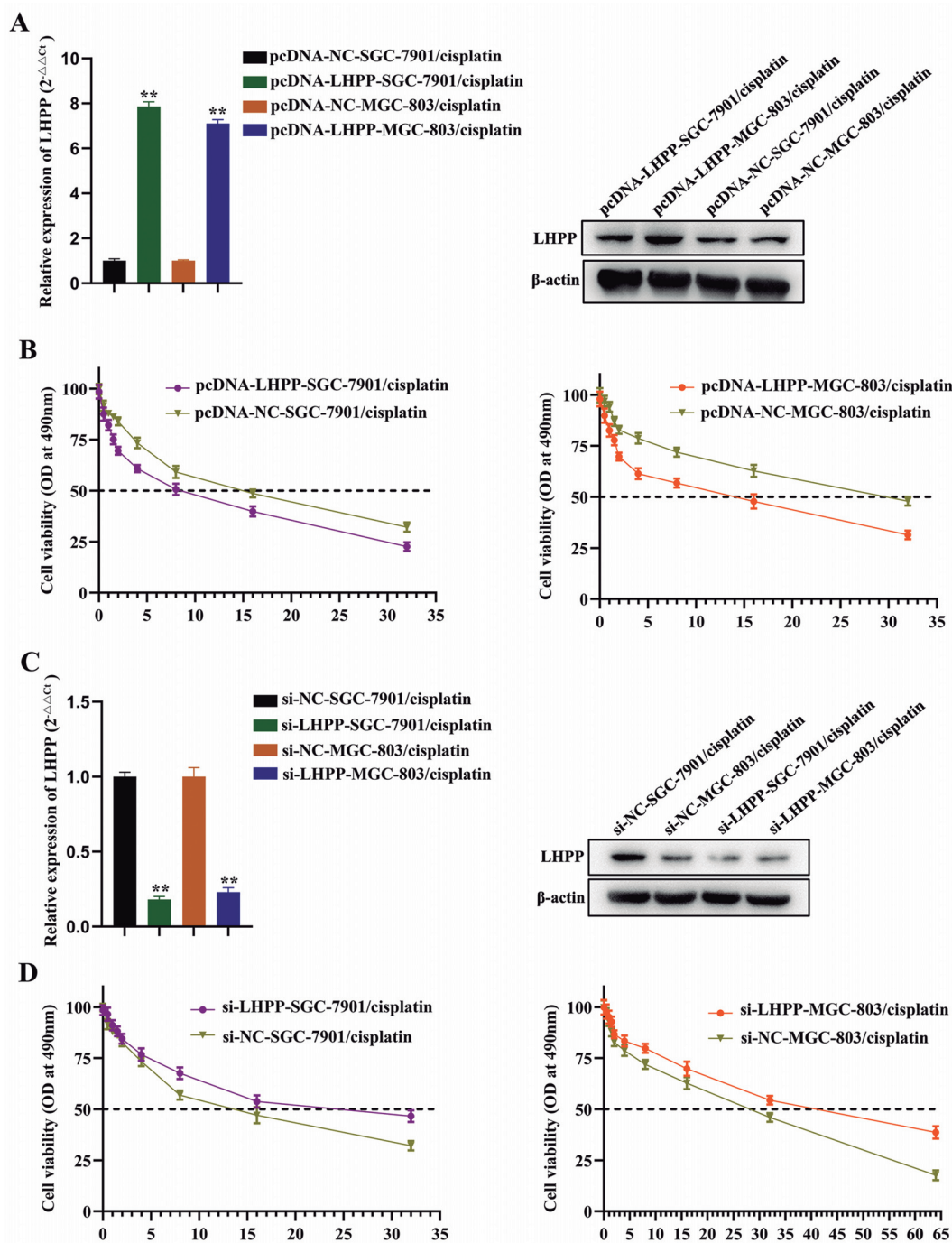

Fig. 4. The effect of LHPP on the sensitivity of SGC-7901/cisplatin and MGC-803/cisplatin cell lines to cisplatin. **A, B.** Compared with the negative control group, SGC-7901/cisplatin and MGC-803/cisplatin cells in the LHPP overexpression expression group were significantly more sensitive to cisplatin. **C, D.** Compared with the negative control group, SGC-7901/cisplatin and MGC-803/cisplatin cells in the si-LHPP group were significantly less sensitive to cisplatin. **P*<0.01, compared to the control group. Data are expressed as mean±standard deviation. OD: optical density; GC: gastric cancer; LHPP: phospholysine phosphohistidine inorganic pyrophosphate phosphatase.

LHPP regulates the intracellular ROS accumulation, stemness, and the sensitivity of SGC-7901/cisplatin and MGC-803/cisplatin GC cells to cisplatin via the JNK and p38 MAPK pathways

To explore the underlying signaling pathways of LHPP in GC, dynamic changes in cell protein were detected by ELISA. The levels of p-p38 and p-JNK were markedly decreased in the pcDNA-LHPP transfection group but largely recovered after si-LHPP cotransfection (Fig. 8A). Moreover, we also found that the intracellular ROS accumulation (Fig. 8B) was observably increased. The above results indicate that the up-regulation of

LHPP may inhibit the JNK and p38 MAPK pathways and promote intracellular ROS accumulation and the sensitivity of SGC-7901/cisplatin and MGC-803/cisplatin GC cells to cisplatin.

Discussion

For the treatment of GC, surgery and radiotherapy are the first and relatively more effective treatments. However, GC patients in some underdeveloped areas are often diagnosed at a later stage and are no longer suitable for surgery. In addition, due to a large number of patients, the waiting time for the radiotherapy machine is
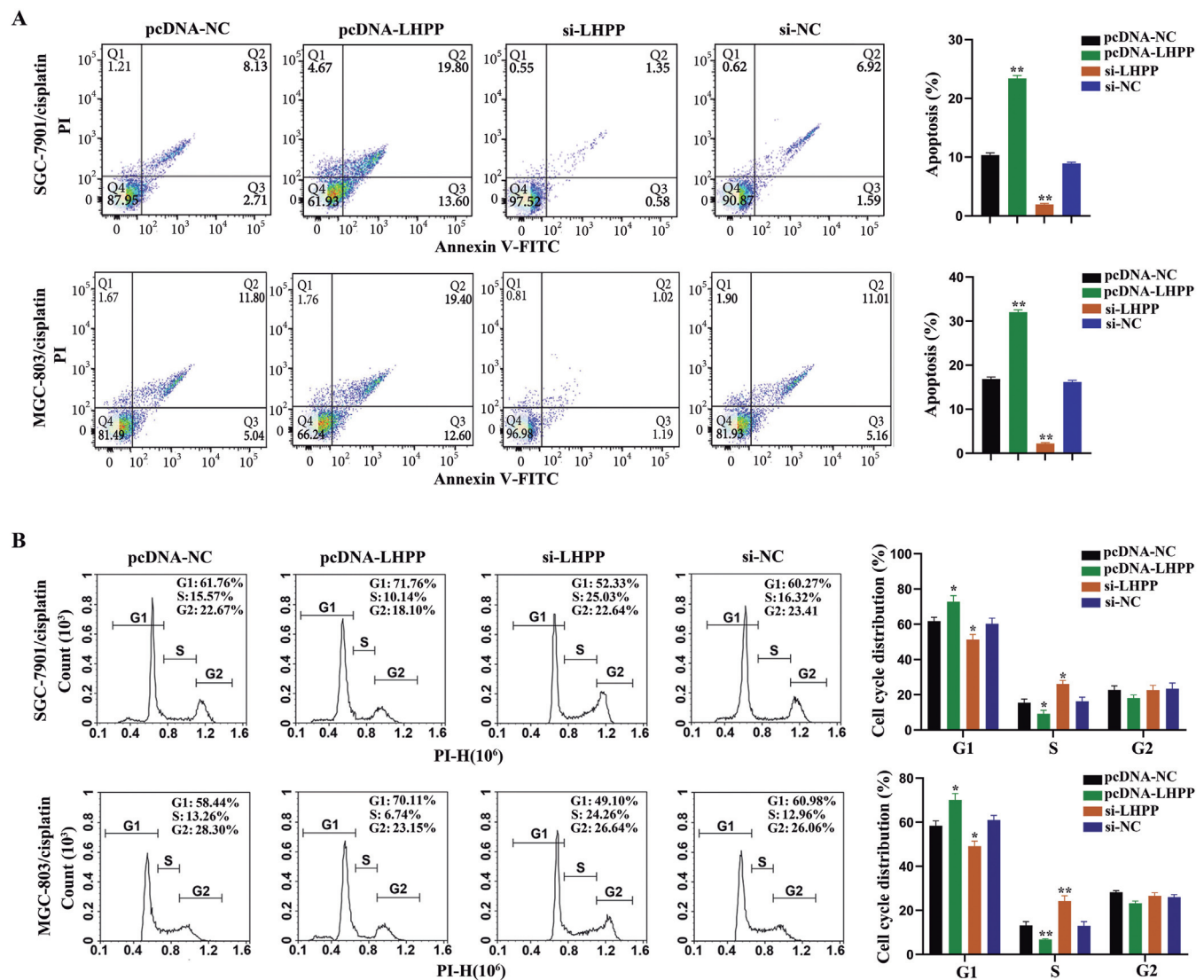

Fig. 5. Up-regulation of LHPP can promote the sensitivity of SGC-7901/cisplatin and MGC-803/cisplatin cell lines to cisplatin. **A.** Cell apoptosis using flow cytometry. **B.** Cell cycle distribution using flow cytometry. *$P<0.05$, compared to the control group; **$P<0.01$, compared to the control group. LHPP: phospholysine phosphohistidine inorganic pyrophosphate phosphatase.
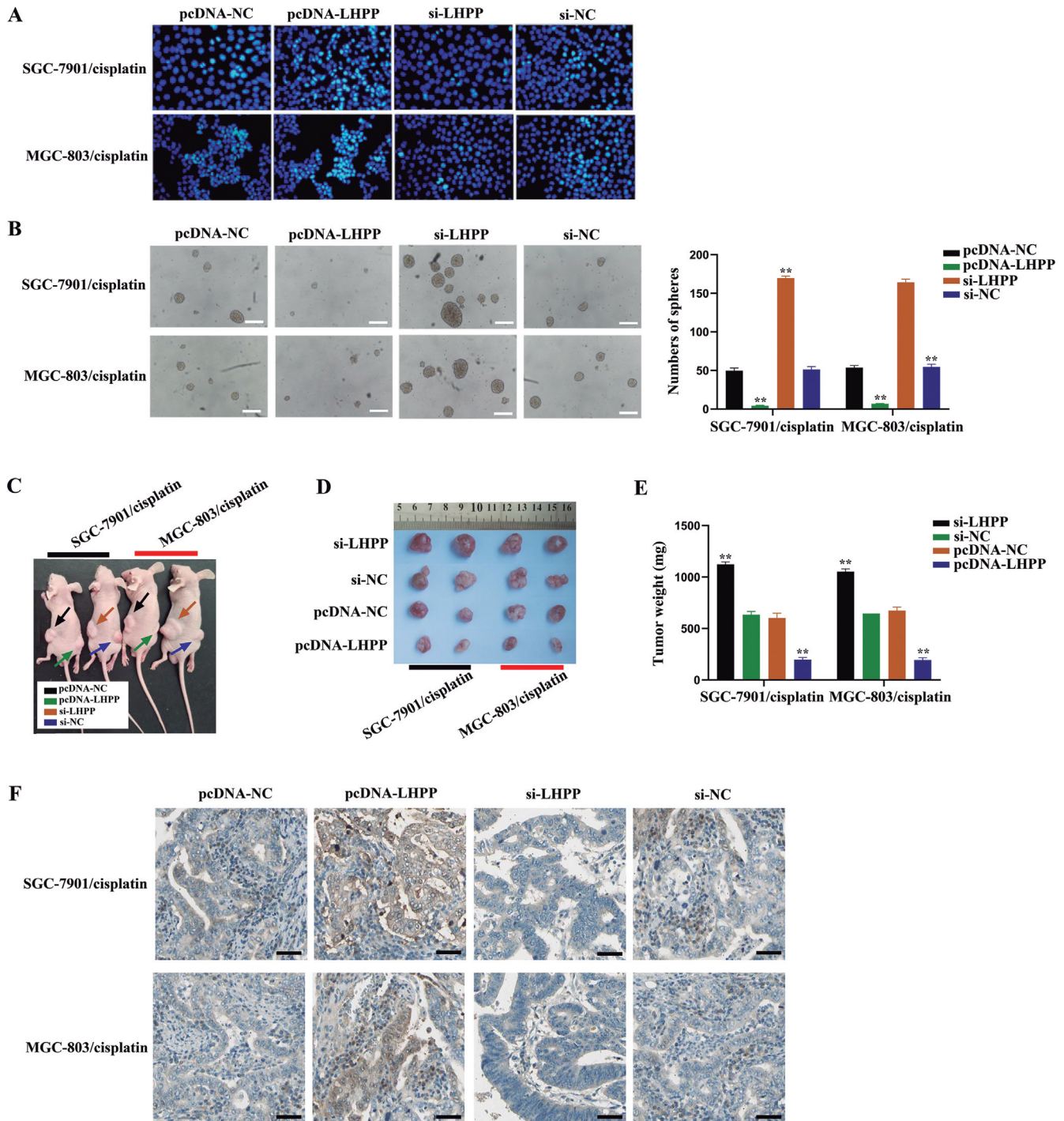
Fig. 6. Up-regulation of LHPP can promote the sensitivity of GC cell lines to cisplatin in vitro and in vivo. **A.** Suppressed cell apoptosis by si-LHPP transfection was observed in SGC-7901/cisplatin and MGC-803/cisplatin cells. **B.** Tumor sphere formation of SGC-7901/cisplatin and MGC-803/cisplatin cells transfected with pcDNA-LHPP cells or si-LHPP. **C-E.** GC nude mouse xenograft tumor model and tumor body. **F.** Immunohistochemical staining of LHPP in tumor-bearing mice. ******P<0.01, compared to the control group. LHPP: phospholysine phosphohistidine inorganic pyrophosphate phosphatase. Scale bars: B, 200 μm; F, 50 μm.

also very long. At present, the combination treatment of surgery and chemoradiotherapy also has not made any further breakthroughs to improve patients' survival rates (Arai et al., 2019). It is worth noting that for patients with advanced GC who have recurrence and metastasis that are not suitable for local treatment, cisplatin-based systemic treatment is often used (Attia and Smyth, 2021). Cisplatin resistance, whether it is inherent resistance or acquired resistance, will seriously affect the effectiveness of treatment. In response to this situation, we have launched a study on how to improve the sensitivity of cisplatin in GC.

In this study, we compared GC tissues from CR and NCR patients by protein chip array and comparison. A total of 338 differentially expressed genes were screened, including 266 up-regulated and 72 down-regulated differentially expressed genes. After PPI network analysis, GEO tissue microarray data, Kaplan-Meier method, and qRT-PCR results, the LHPP protein was finally determined. LHPP protein contains ubiquitin

protein action motifs, which can mediate the degradation of ubiquitinated proteins. In the process of protein metabolism and degradation, ubiquitin transporters are believed to promote the degradation of ubiquitin proteins (Chen et al., 2021). However, related studies have shown that the ubiquitin-proteasome system is also inhibited by ubiquitin transporters (Walters et al., 2002; Liang et al., 2014). Cell experiments found that LHPP impedes glycolysis and respiration during the energy metabolic process, and mouse experiments showed that the

Table 2. The fold change on each protein individually between the down-expression of LHPP and control groups.

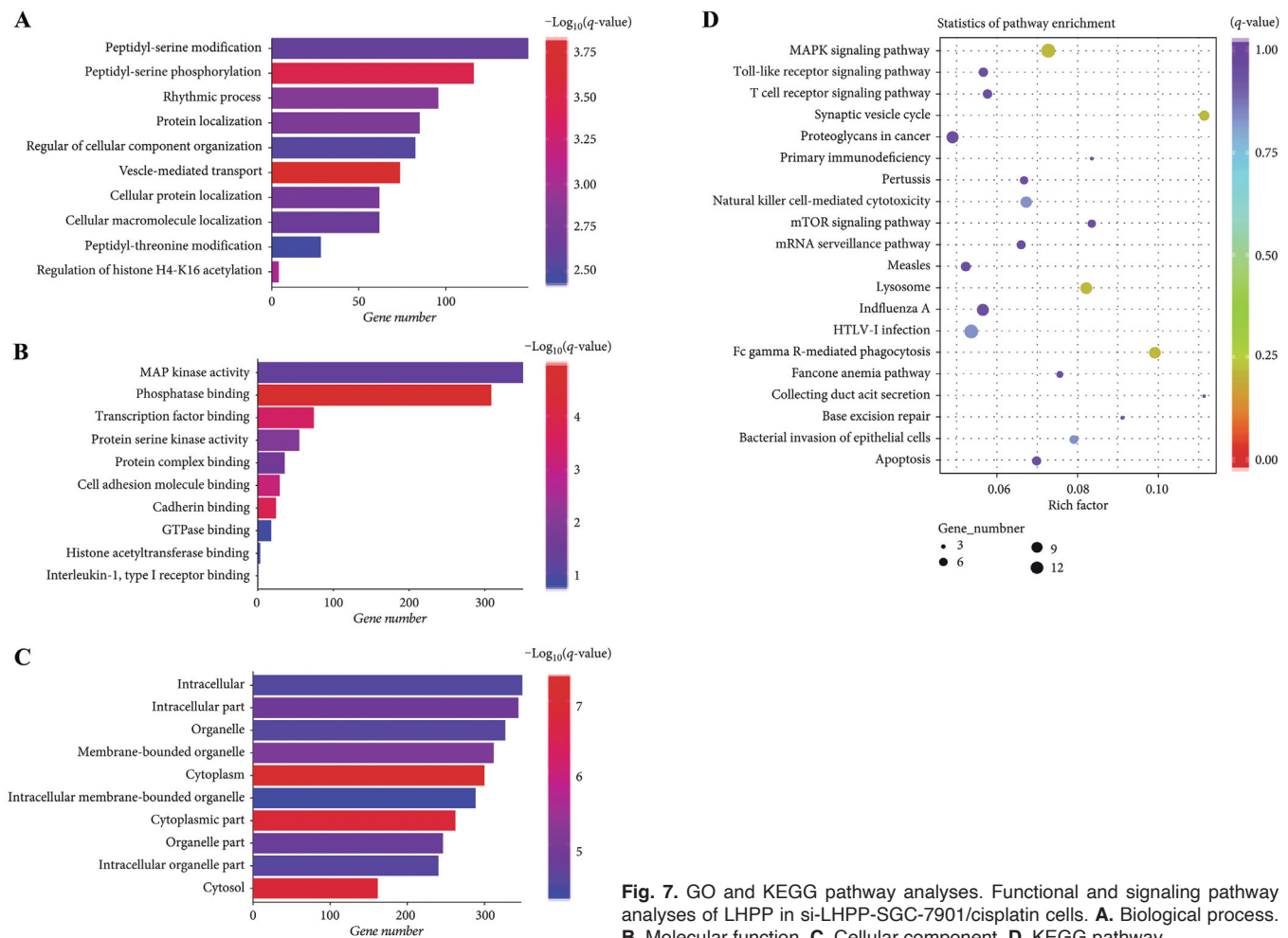| Proteins	Mean CTL	Mean OE	Fold change
p38	3228.087	5873.165	1.8193949
JNK	3154.982	4159.866	1.3185070

Fig. 7. GO and KEGG pathway analyses. Functional and signaling pathway analyses of LHPP in si-LHPP-SGC-7901/cisplatin cells. **A.** Biological process. **B.** Molecular function. **C.** Cellular component. **D.** KEGG pathway.

degradation of p53 and IκB molecules in cells was inhibited by AKT, and there was an interaction between LHPP and p53 and AKT (Zheng et al., 2018). A recent study has found that the interaction between the proteasome and the ubiquitin-binding protein PKM2 is affected by LHPP, thereby acting on the ubiquitin-proteasome degradation system (Chen et al., 2021). LHPP can also be hydrolyzed into small fragments and then secreted out of the cell, participating in a variety of biological processes, suggesting that the role of LHPP in tumors is complex (Hauser et al., 2020).

Yang et al. (2021) found that GAS5 inhibited NSCLC cisplatin resistance by attenuating the endogenous effect of miR-217, thereby promoting LHPP mRNA and protein expression. However, there is no report on whether LHPP is involved in cisplatin resistance in GC. To prove the relationship between LHPP expression and cisplatin sensitivity of GC, in this study, we used an MTT assay to detect the survival of LHPP low- (si-LHPP) and over-expressing (pcDNA-LHPP) cells under the action of cisplatin. We found that, compared with the parental GC cells, the survival rate was markedly reduced in the LHPP over-expressing cells, and evidently increased in the si-LHPP cotransfection cells. We then used flow cytometry to compare the apoptosis changes of cisplatin-induced LHPP low- and over-expressing cells and control cells. It was found that the apoptotic rate of cells with high LHPP expression increased significantly, and the results of Hoechst staining and tumor sphere formation assay

also proved that the overexpression of LHPP enhanced cell nuclear fragmentation, and inhibited the capacity to form spheres. At the same time, the results of in vivo animal experiments also showed that the growing volume and rate of LHPP down-regulated mouse tumors after cisplatin treatment were significantly higher than those in the control group, while the sensitivity of nude mice with high LHPP expression to cisplatin increased markedly. These results indicate that the overexpression of LHPP can promote the cisplatin sensitivity of GC cells. The positive effect of LHPP in improving the chemotherapy sensitivity of tumor patients has been confirmed in some studies (Zhang et al., 2019; Li et al., 2021; Yang et al., 2021).

To further explore the mechanism of LHPP in enhancing the cisplatin sensitivity of GC, we sequenced si-LHPP-SGC-7901/cisplatin and si-NC-SGC-7901/cisplatin GC cells. Our results found that differentially expressed genes were mainly enriched in the MAPK signaling pathway. A previous study has demonstrated that adding cisplatin to GC BGC-823 and SGC-7901 cells can inhibit the MAPK signaling pathway and down-regulate the expression of MAPK3 (Chen et al., 2019). Our western blot results validated that the up-regulated genes after transfecting with pcDNA-LHPP in GC cells were involved in the MAPK signaling pathway, in which the p38 and JNK pathways are involved to regulate tumor cell physiology and are also found to be activated in GC. We believe that the continuously inactivated p38 and JNK may provide mechanisms to
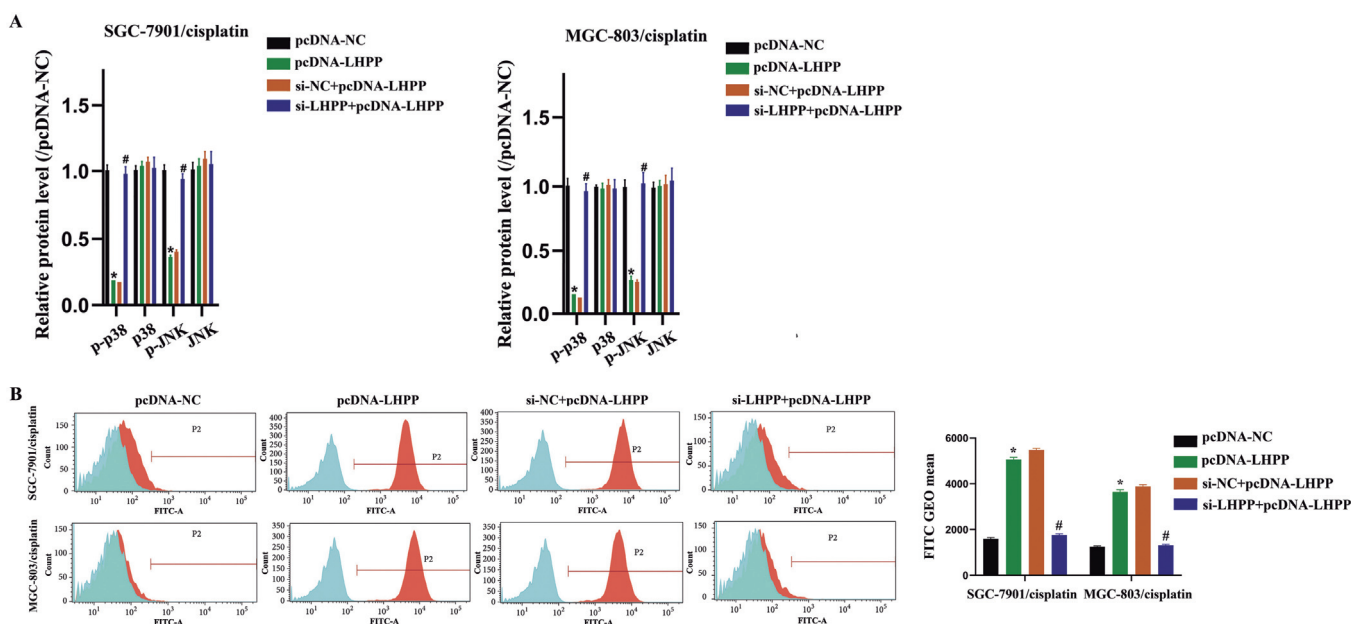

Fig. 8. The p38 and JNK MAPK pathways were involved in LHPP-regulated intracellular ROS accumulation and the sensitivity of SGC-7901/cisplatin and MGC-803/cisplatin GC cells. **A.** SGC-7901/cisplatin and MGC-803/cisplatin cells were transfected with the pcDNA-NC, pcDNA-LHPP, si-NC, and si-LHPP. ELISA was performed. **B.** Flow cytometry was used to detect the level of ROS in SGC-7901/cisplatin and MGC-803/cisplatin GC cells transfected with pcDNA-LHPP cells or si-LHPP.

promote GC cell apoptosis. Studies have validated the potential interactions between the MAPK signaling pathway and ROS (Hu et al., 2019; Sheng et al., 2020; Cao et al., 2021). The transcription of MAPK signaling pathway-dependent genes can affect the accumulation of ROS in tumor cells. A current study has demonstrated that the MAPK signaling pathway was associated with ROS-induced nonapoptotic programmed cell death in hepatocellular carcinoma (Chang et al., 2021). In this study, we found that compared with the control group, over-expressing LHPP can promote cisplatin-induced apoptosis, indicating that the sensitivity of GC cells to cisplatin may be closely related to ROS. Our inference is also supported by previous literature reports (Chang et al., 2021). Therefore, we speculate that inhibition of the JNK and p38 MAPK pathways may promote the accumulation of ROS in GC-resistant cells induced by cisplatin, thereby inducing GC cell apoptosis.

In summary, the up-regulation of LHPP may inhibit the activation of the JNK and p38 MAPK pathways, attenuate stemness, and enhance the accumulation of intracellular ROS, thereby promoting cisplatin-mediated GC cell apoptosis and enhancing cisplatin sensitivity. Our study may provide new theoretical bases for cisplatin sensitivity and chemotherapy in GC patients. At the same time, LHPP and JNK and p38 MAPK pathway-related genes may become prognostic targets for cisplatin therapy for GC patients.

References

Arai H., Iwasa S., Boku N., Kawahira M., Yasui H., Masuishi T., Muro K., Minashi K., Hironaka S., Fukuda N., Takahari D. and Nakajima T.E. (2019). Fluoropyrimidine with or without platinum as first-line chemotherapy in patients with advanced gastric cancer and severe peritoneal metastasis: a multicenter retrospective study. BMC. Cancer 19, 652.

Attia H. and Smyth E. (2021). Evolving therapies in advanced oesophago-gastric cancers and the increasing role of immunotherapy. Expert. Rev. Anticancer Ther. 21, 535-546.

Cai S., Bai Y., Wang H., Zhao Z., Ding X., Zhang H., Zhang X., Liu Y., Jia Y., Li Y., Chen S., Zhou H., Liu H. Yang C. and Sun T. (2020). Knockdown of THOC1 reduces the proliferation of hepatocellular carcinoma and increases the sensitivity to cisplatin. J. Exp. Clin. Cancer Res. 39, 135.

Cao X., Fu M., Bi R., Zheng X., Fu B., Tian S., Liu C., Li Q. and Liu J. (2021). Cadmium induced BEAS-2B cells apoptosis and mitochondria damage via MAPK signaling pathway. Chemosphere 263, 128346.

Chang W.T., Bow Y.D., Fu P.J., Li C.Y., Wu C.Y., Chang Y.H., Teng Y.N., Li R.N., Lu M.C., Liu Y.C. and Chiu C.C. (2021). A marine terpenoid, heteronemin, induces both the apoptosis and ferroptosis of hepatocellular carcinoma cells and involves the ROS and MAPK pathways. Oxid. Med. Cell Longev. 2021, 7689045.

Chen Z., Gao Y.J., Hou R.Z., Ding D.Y., Song D.F., Wang D.Y. and Feng Y. (2019). MicroRNA-206 facilitates gastric cancer cell apoptosis and suppresses cisplatin resistance by targeting MAPK2 signaling pathway. Eur. Rev. Med. Pharmacol. Sci. 23, 171-180.

Chen W.J., Chen L.H., Wang J., Wang Z.T., Wu C.Y., Sun K., Ding B.Y., Liu N. and Xu R.X. (2021). LHPP impedes energy metabolism by inducing ubiquitin-mediated degradation of PKM2 in glioblastoma. Am. J. Cancer Res. 11, 1369-1390.

Chiu C.F., Weng J.R., Lee S.L., Wu C.Y., Chu P.C., Shan Y.S., Yang H.R. and Bai L.Y. (2020). OSU-A9 induced-reactive oxygen species cause cytotoxicity in duodenal and gastric cancer cells by decreasing phosphorylated nuclear pyruvate kinase M2 protein levels. Biochem. Pharmacol. 174, 113811.

Hauser A., Hwang S., Sun H. and Hackenberger C. (2020). Combining free energy calculations with tailored enzyme activity assays to elucidate substrate binding of a phospho-lysine phosphatase. Chem. Sci. 11, 12655-12661.

Hindupur S.K., Colombi M., Fuhs S.R., Matter M.S., Guri Y., Adam K., Cornu M., Piscuoglio S., Ng C., Betz C., Liko D., Quagliata L., Moes S., Jenoe P., Terracciano L.M., Heim M.H., Hunter T. and Hall M.N. (2018). The protein histidine phosphatase LHPP is a tumour suppressor. Nature 555, 678-682.

Hu S., Huang J., Pei S., Ouyang Y., Ding Y., Jiang L., Lu J., Kang L., Huang L., Xiang H., Xiao R., Zeng Q. and Chen J. (2019). *Ganoderma lucidum* polysaccharide inhibits UVB-induced melanogenesis by antagonizing cAMP/PKA and ROS/MAPK signaling pathways. J. Cell Physiol. 234, 7330-7340.

Kamimura K., Suda T., Fukuhara Y., Okuda S., Watanabe Y., Yokoo T., Osaki A., Waguri N., Ishikawa T., Sato T., Aoyagi Y., Takamura M., Wakai T. and Terai S. (2021). Adipose most abundant 2 protein is a predictive marker for cisplatin sensitivity in cancers. Sci. Rep. 11, 6255.

Koken E., Oyar E.O., Uyanikgil Y., Pazarlar B.A., Bilister C., Aksun S., Yigitturk G. and Koken E.C. (2020). Exogenous follistatin administration ameliorates cisplatin-induced acute kidney injury through anti-inflammation and anti-apoptosis effect. Bratisl. Lek. Listy. 121, 143-150.

Kurtzeborn K., Kwon H. N. and Kuure S. (2019). MAPK/ERK signaling in regulation of renal differentiation. Int. J. Mol. Sci. 20, 1779.

Lee S., Rauch J. and Kolch W. (2020). Targeting MAPK signaling in cancer: Mechanisms of drug resistance and sensitivity. Int. J. Mol. Sci. 21, 1102.

Li Y., Zhang X., Zhou X. and Zhang X. (2019). LHPP suppresses bladder cancer cell proliferation and growth via inactivating AKT/p65 signaling pathway. Biosci. Rep. 39, BSR20182270.

Li Z., Zhou X., Zhu H., Song X., Gao H., Niu Z. and Lu J. (2021). Purpurin binding interacts with LHPP protein that inhibits PI3K/AKT phosphorylation and induces apoptosis in colon cancer cells HCT-116. J. Biochem. Mol. Toxicol. 35, e22665.

Liang R.Y., Chen L., Ko B.T., Shen Y.H., Li Y.T., Chen B.R., Lin K.T., Madura K. and Chuang S. M. (2014). Rad23 interaction with the proteasome is regulated by phosphorylation of its ubiquitin-like (UbL) domain. J. Mol. Biol. 426, 4049-4060.

Peng L., Sang H., Wei S., Li Y., Jin D., Zhu X., Li X., Dang Y. and Zhang G. (2020). circCUL2 regulates gastric cancer malignant transformation and cisplatin resistance by modulating autophagy activation via miR-142-3p/ROCK2. Mol. Cancer 19, 156.

Sexton R.E., Al Hallak M.N., Diab M. and Azmi A.S. (2020). Gastric cancer: a comprehensive review of current and future treatment strategies. Cancer Metastasis Rev. 39, 1179-1203.

Sheng Y.N., Luo Y.H., Liu S.B., Xu W.T., Zhang Y., Zhang T., Xue H., Zuo W.B., Li Y.N., Wang C.Y. and Jin C.H. (2020). Zeaxanthin induces apoptosis via ROS-regulated MAPK and AKT signaling pathway in human gastric cancer cells. Onco Targets Ther. 13, 10995-11006.

Sun W., Qian K., Guo K., Chen L., Xiang J., Li D., Wu Y., Ji Q., Sun T. and Wang Z. (2020). LHPP inhibits cell growth and migration and triggers autophagy in papillary thyroid cancer by regulating the AKT/AMPK/mTOR signaling pathway. Acta. Biochim. Biophys. Sin. (Shanghai) 52, 382-389.

Sung H., Ferlay J., Siegel R.L., Laversanne M., Soerjomataram I., Jemal A. and Bray F. (2021). Global Cancer Statistics 2020: GLOBOCAN Estimates of Incidence and Mortality Worldwide for 36 Cancers in 185 Countries. CA. Cancer J. Clin. 71, 209-249.

Walters K.J., Kleijnen M.F., Goh A.M., Wagner G. and Howley P.M. (2002). Structural studies of the interaction between ubiquitin family proteins and proteasome subunit S5a. Biochemistry 41, 1767-1777.

Wang J., Deng H., Zhang J., Wu D., Li J., Ma J. and Dong W. (2020a). α-Hederin induces the apoptosis of gastric cancer cells accompanied by glutathione decrement and reactive oxygen species generation via activating mitochondrial dependent pathway. Phytother. Res. 34, 601-611.

Wang J., Han C., Lu Z., Ge P., Cui Y., Zhao D., Yang X., Wu B., Qiang L., Zhang Y., Chai Q., Lei Z., Li L., Hua Liu C. and Zhang L. (2020b). Simulated microgravity suppresses MAPK pathway-mediated innate immune response to bacterial infection and induces gut microbiota dysbiosis. FASEB J. 34, 14631-14644.

Wu F., Chen Y. and Zhu J. (2020). LHPP suppresses proliferation, migration, and invasion and promotes apoptosis in pancreatic cancer. Biosci. Rep. 40, BSR20194142.

Yang X., Meng L., Zhong Y., Hu F., Wang L. and Wang M. (2021). The long intergenic noncoding RNA GAS5 reduces cisplatin-resistance in non-small cell lung cancer through the miR-217/LHPP axis. Aging (Albany NY) 13, 2864-2884.

Zhang Q., Xiong M., Liu J., Wang S., Du T., Kang T., Liu Y., Cheng H., Huang M. and Gou M. (2019). Targeted nanoparticle-mediated LHPP for melanoma treatment. Int. J. Nanomedicine 14, 3455-3468.

Zhang F., Wang H., Yu J., Yao X., Yang S., Li W., Xu L. and Zhao L. (2021). LncRNA CRNDE attenuates chemoresistance in gastric cancer via SRSF6-regulated alternative splicing of PICALM. Mol. Cancer 20, 6.

Zhao F., Vakhrusheva O., Markowitsch S.D., Slade K.S., Tsaur I., Cinatl J., Jr Michaelis M., Efferth T., Haferkamp A. and Juengel E. (2020a). Artesunate impairs growth in cisplatin-resistant bladder cancer cells by cell cycle arrest, apoptosis and autophagy induction. Cells 9, 2643.

Zhao P., Cui X., Zhao L., Liu L. and Wang D. (2020b). Overexpression of growth-arrest-specific transcript 5 improved cisplatin sensitivity in hepatocellular carcinoma through sponging miR-222. DNA Cell Biol. 39, 724-732.

Zheng J., Dai X., Chen H., Fang C., Chen J. and Sun L. (2018). Down-regulation of LHPP in cervical cancer influences cell proliferation, metastasis and apoptosis by modulating AKT. Biochem. Biophys. Res. Commun. 503, 1108-1114.

Zhu G., Shen Q., Jiang H., Ji O., Zhu L. and Zhang L. (2020). Curcumin inhibited the growth and invasion of human monocytic leukaemia SHI-1 cells in vivo by altering MAPK and MMP signalling. Pharm. Biol. 58, 25-34.